

MICROCOPY RESOLUTION TEST CHART
NATIONAL BUREAU OF STANDARDS 1964 A

AD-A151 397

	to Entered) MASTE	R COPY - FOR REPRODUCTION P	
REPORT DOCUMENTATION	PEAD INSTPUCTIONS BEFORE COMPLETING FORM		
I. REPORT NUMBER	2. GOVT ACCESSION NO.		
ARO 18978.6.CH	N/A	N/A	
4. TITLE (and Subtitio)		5. TYPE OF REPORT & PERIOD COVERED	
Ionic Conductivity and Microwav Relaxation of LiAsF <sub>6</sub> and LiClO	Technical		
Dimethylcarbonate		6. PERFORMING ORG. REPORT NUMBER	
7. AUTHOR(a)		8. CONTRACT OR GRANT NUMBER(+)	
Marta Delsignore, Herman Farl Sergio Petrucci	ber and	DAAG-29-82-K0048	
Polytechnic Institute of New Yor Department of Chemistry, Long Route 110, Farmingdale, New Y	rk ; Island Center	10. PROGRAM CLEMENT, PROJECT, TASK ARLA & WORK UNIT NUMBERS	
11. CONTROLLING OFFICE NAME AND ADDRESS		12. REPORT DATE	
U. S. Army Research Office		January 1985	
Post Office Box 12211		January 1985 13. NUMBER OF PAGES	
Research Triumple Pork NC 2770	orent from Controlling Office)	15. SECURITY CLASS, (of this report)	
		Unclassified	
·		15a, DECLASSIFICATION/DOWNGRADING SCHEDULE	
Approved for public release; di	stribution unlimit	DTIC ELECTE MAR 1 9 1985	
		MAR 1 9 1985	

18. SUPPLEMENTARY NOTES

The view, opinions, and/or findings contained in this report are those of the author(s) and should not be construed as an official Department of the Army position, policy, or decision, unless so

designated by other documentation.

19. KEY WORDS (Continue on reverse state to necessary and identity by block number)

Electrical conductance, microwave dielectric relaxation, LiAsF<sub>6</sub>, Dimethylcarbonate.

23. AUGIFACT (Conthum we reverse slide if in connery and identify by block comber)

Audiofrequency electrical conductivity data are reported in the solvent dimethylcarbonate (DMC) at 25°C in the concentration range  $10^{-4}$  to 1M for LiAsF6 and  $10^{-4}$  to 0.3M for LiClO<sub>4</sub>. From  $10^{-4}$  to  $\approx 10^{-2}$ M the data are interpreted by the Fuoss-Kraus triple-ions theory leading to the values of the ion pair formation constant K<sub>n</sub> and triple ion formation constant K<sub>T</sub>. For the data at higher concentration, it is shown that the change of static permittivity of the solution (due to the presence of solute ion-pairs and other polar species, which increase the polarization of the solution) can account

55 1 JAN 73 1473

EDITION OF 1 NOV 65 IS ODSOLETE

UNCLASSITIED

85 07

qualitatively for the behavior of the conductance data and their derivation from the Fuoss-Kraus theory. In other words, these deviations are mostly due to changes in permittivity, not accounted for in the conventional treatment of the data, rather than by the failure of the theory, which is better than recognized so far. Introduction of the quadrupole formation constant is necessary, however, for LiAsF6 for a more quantitative treatment of the conductance data. Microwave complex permittivities in the concentration range 0.05M to 0.3M, frequency range  $\approx 1$  to 90 GHz are interpreted by two Debye relaxation processes, one due to the solute and one to the solvent. For LiAsF6 the Bottcher plot (expressing a quantity related to the change of the relaxation strength ( $\varepsilon_0$ - $\varepsilon_{001}$ ) with the concentration of electrolyte) is

nonlinear with concentration. Correction of the concentration, by postulating the presence of dielectrically apolar dimers linearizes the plot with a quadrupole formation constant of the order of  $K_q \approx 50 M^{-1}$ , although this figure is very tentative. For LiAsF6 both rotational relaxation time and the distance separation of the charges as calculated from the apparent dipole moment suggest distances of the order of contact ion pairs. For LiClO<sub>4</sub> no curvature in the Bottcher plot is visible, suggesting that presence of quadrupoles is not significant for this electrolyte in DMC, a notion already reported in the literature. This is somewhat surprising in view of the ionic association constant to pairs  $K_p$ , being an order of magnitude larger for LiClO<sub>4</sub> with respect to LiAsF6. The distance separation of the charges, as calculated from the apparent dipole moment of LiClO<sub>4</sub> suggests presence of contact species.

Acce	ssion For	
	GRASI	3
DIIC		4
Ulina	Berlynoa j	
វិមេមដ	Made Made	
P	ta a a	
$\mathbf{D} \subseteq \mathbb{N}$	Mark Say	
	ikanin <del>,</del> c	· · · · · · · · · · · · · · · · · · ·
in i	$(a_1, a_2) = 2a_1 + a_2 a_2$	Or
. i. L	Theorial	
<b>A</b> 1	,	
4-1	i ]	
	, 1	

### Ionic Conductivity and Microwave Dielectric Relaxation of LiAsF<sub>6</sub> and LiClO<sub>4</sub> in Dimethylcarbonate

bу

M. Delsignore,\* H. Farber and S. Petrucci

Department of Chemistry and Department of Electrical Engineering

Long Island Center

Polytechnic Institute of New York

Route 110

Farmingdale, NY 11735

#### ABSTRACT

Audiofrequency electrical conductivity data are reported in the solvent dimethylcarbonate (DMC) at 25°C in the concentration range  $10^{-4}$  to 1M for LiAsF<sub>6</sub> and  $10^{-4}$  to 0.3M for LiClO<sub>4</sub>. From  $10^{-4}$  to  $\approx 10^{-2}$ M the data are interpreted by the Fuoss-Kraus triple-ions theory leading to the values of the ion pair formation constant  $K_p$  and triple ion formation constant  $K_T$ . For the data at higher concentration, it is shown that the change of static permittivity of the solution (due to the presence of solute ion-pairs and other polar species, which increase the polarization of the solution) can account qualitatively for the behavior of the conductance data and their derivation from the Fuoss-Kraus theory. In other words, these deviations are mostly due to changes in permittivity, not accounted for in the conventional treatment of the data, rather than by the failure of the theory, which is better than recognized so far. Introduc-

Present address: Colgate-Palmolive Co., Piscataway, New Jersey.

tion of the quadrupole formation constant is necessary, however, for LiAsF<sub>6</sub> for a more quantitative treatment of the conductance data. Microwave complex permittivities in the concentration range 0.05M to 0.3M, frequency range  $\approx 1$ to 90 GHz are interreted by two Debye relaxation processes, one due to the solute and one to the solvent. For LiAsF<sub>6</sub> the Bottcher plot, (expressing a quantity related to the change of the relaxation strength  $(\epsilon_0 - \epsilon_{001})$  with the concentration of electrolyte), is nonlinear with the concentration. Correction of the concentration, by postulating the presence of dielectrically apolar dimers linearizes the plot with a quadrupole formation constant of the order of  $K_{\text{q}}{\approx}50\text{M}^{-1}\text{,}$  although this figure is very tentative. For LiAsF  $_{6}$  both rotational relaxation time and the distance separation of the charges as calculated from the apparent dipole moment suggest distances of the order of contact ion pairs. For LiClO<sub>4</sub> no curvature in the Böttcher plot is vis ble, suggesting that presence of quadrupoles is not significant for this electrolyte in DMC, a notion already reported in the literature. This is somewhat surprising in view of the ionic association constant to pairs K<sub>p</sub>, being an order of magnitude larger for LiClO<sub>4</sub> with respect to LiAsF<sub>6</sub>. The distance separation of the charges, as calculated from the apparent dipole moment of LiClO4 suggests presence of contact species.

#### Introduction

Research with the electrochemically relevant electrolyte LiAsF<sub>6</sub> has been carried out so far, in this laboratory, in the ethereal solvents 1,2-DME<sup>1</sup> and 2-MethylTIF<sup>2</sup> of respective permittivities  $\epsilon$ =7.05 and  $\epsilon$ =6.2. This electrolyte shows a high solubility (>1M) in the solvent dimethylcarbonate of  $\epsilon$ =3.1<sup>3</sup>. Due to its higher electrolyte strength with respect to LiClO<sub>4</sub>, a perhaps due to steric and donicity properties of AsF<sub>6</sub> it was thought quite relevant to carry a parallel investigation of LiAsF<sub>6</sub> and liClO<sub>4</sub> in DMC also because of the rare chance to extend to high electrolyte concentrations, a study in a medium of such low permittivity. Two experimental methods, audiofrequency electrical conductivity and microwave coaxial and rectangular waveguide reflectometry (leading to the determination of the complex permittivity  $\epsilon$ \*= $\epsilon$ '- J $\epsilon$ ") have been used at the temperature t=25°C. The present work also extends to higher concentrations of LiClO<sub>4</sub>, some microwave work reported earlier.<sup>3</sup>

#### Experimental Part

LiAsF<sub>6</sub> (Agri Chem. Co., Atlanta, Georgia) and LiClO<sub>4</sub> (C. P. Smith Co., Cleveland, Ohio) were dried at 70° in vacuo overnight. Dimethylcarbonate (Aldrich Chemical Co., 99% product) was distilled twice in a cell pyrex Vigreaux column without grease on the joints. A portion of DMC was dried over activated  $4\mathring{\Lambda}$  molecular sieves and distilled over them (about 1/5 of volume of sieves with respect to the liquid). The molecular sieves were dried at  $\approx$ 100°C in vacuo overnight. A conductivity run for LiAsF<sub>6</sub> in DMC distilled over molecular sieves gave same results as for DMC distilled without molecular sieves. For the microwave work, solutions were kept in dessicators. Contact with open atmosphere was kept to a few seconds, namely, the time necessary to fill the cells. The equipment for the conductance work has been extensively described. The setups for the microwave work has been reported in previous

papers.<sup>3,6,7</sup> The only change of significance has been in the automation and digitization of data capturing. Specifically, the 1000 Hz modulated signal from the crystal detectors is now fed to a Hewlett-Packard 3408A digital voltmeter which is sensitive to  $\pm 1\mu V$ . The meter is part of a loop comprising a Hewlett-Packard 41CV calculator a HP-82160A-1L interface and a HP82162A thermal printer. The ac modulated voltage is transmitted to the calculator upon pressing a command that induces the calculator to "listen" to the voltmeter. The calculator in turn "talks" to the printer giving the decimal log of the digitized voltage which gets hard copied. The micrometric measurements of the reflector have also been motorized with the result that the system is a semiautomatic reflectometer recording the db vs. distance of the reflector receding from the mica window holding the liquid at the bottom of the coaxial line (1-4 GHz) or of various waveguides (8-90 GHz).

#### Results and Discussion

#### a) Electrical Conductance

Table I reports the equivalent electrical conductivities  $\Lambda(\Omega^{-1} \text{cm}^2 \text{eq}^{-1})$  and the molar concentration c (M) for LiAsF<sub>6</sub> in DMC at 25°C. Four runs were performed with two conductance cells of cell constant  $K_c=0.1156\text{cm}^{-1}$  and  $K_c=0.2794\text{cm}^{-1}$ . This last cell was used for Run #4 at c > 0.5M. The cell of lower constant was recalibrated with recrystalized KCl dissolved in water, measuring the cell impedance in the frequency range 1000, 5000 Hz and using the Fuoss et al. equation<sup>8</sup> for the cell calibration:

$$\Lambda = 149.93 - 94.65c^{1/2} + 58.74 cloge + 198.4c.$$

The result over five solutions was

$$K_c = (0.1156 \pm 0.0004) \text{ cm}^{-1}$$

Fig. 1 shows the same data in the form of  $\log_{10}\Lambda$  vs.  $\log_{10}c$ . A dramatic

change, over several order of magnitudes for  $\Lambda$ , changing with concentration, takes place. Clearly, at  $\approx 1 \mathrm{M}$  we have a conductivity comparable to the one of LiAsF<sub>6</sub> in DME at  $c \approx 10^{-4} \mathrm{M}$ , a not too surprising event if one realizes that the permittivity of the solution has increased dramatically from  $\epsilon = 3.1$ , the value of the solvent, as shown below. In the range of electrolyte concentration  $10^{-4}$  to  $10^{-2} \mathrm{M}$ , the classical Fuoss-Kraus theory for triple-ion formation<sup>9</sup> reads

$$\Lambda g(c)\sqrt{c} = \frac{\Lambda_o}{\sqrt{i\zeta_p}} + \frac{\Lambda_T^o K_T}{\sqrt{i\zeta_p}} \left(1 - \frac{\Lambda}{\Lambda_o}\right)c \tag{I}$$

with

$$g(c) = \frac{\exp(-2.303 \frac{\beta'}{\Lambda_o^{1/2}} \sqrt{c} \Lambda)}{(1 - \frac{S}{\Lambda_o^{3/2}} \sqrt{c} \Lambda)(1 - \frac{\Lambda}{\Lambda_o})^{1/2}}$$

where  $\beta'$  is the Debye-Huckel activity coefficient term

$$\beta' = \frac{1.8247 \times 10^6}{(\epsilon T)^{3/2}}$$

and

$$S = \alpha \Lambda_o + \beta = \frac{0.8204 \times 10^6}{(\epsilon T)^{3/2}} \Lambda_o + \frac{82.501}{\eta (\epsilon T)^{1/2}}$$

is the Onsager conductance term. We have used  $\epsilon=3.12,\,\eta=0.00585,\,$  and  $\Lambda_o(\text{LiAsF}_6)=97.4,\,\Omega^{-1}\text{cm}^2\text{eq}^{-1},\,$  based on  $\Lambda_o=22.53$  in propylenecarbonate,  $\eta=0.0253\text{p}$  and the Walden rule. The results, applying Eq. 1 to the data, are determination coefficient  $r^2=0.988,\,$  Intercept =  $1.033\text{x}\,10^{-4},\,$  Slope =  $0.0306,\,$  from which  $K_p=8.9\text{x}\,10^{11}\,$  M<sup>-1</sup> and  $K_T=445\text{M}^{-1},\,$  having chosen the arbitrary position  $\Lambda_T^o=\frac{2}{3}\,\Lambda^o$  as done previously. Fig. 2 reports an illustration of function (I) for the present data.

Figs. 3a shows the  $\log_{10}\Lambda$  data for LiClO<sub>4</sub> in DMC at 25°, plotted vs.  $\log_{10}c$ . Table I reports the  $\Lambda$  and c data for the two runs performed for LiClO<sub>4</sub> in DMC at 25°C. One can see immediately by comparing Figs. 1 and 3 that the equivalent conductance of LiClO<sub>4</sub> is one order of magnitude lower than that of LiAsF<sub>6</sub> at the same total concentration. Application of Eq. (1) to the data at  $c<10^{-2}M$  for LiClO<sub>4</sub> is shown in Fig. 3b. Linear regressions of  $\Lambda g(c)\sqrt{c}$  vs.  $c(1-\frac{\Lambda}{\Lambda_o})$  gives  $r^2=0.993$ , Intercept = 0.3937x10<sup>-4</sup>, Slope = 0.0110, from which  $K_p=8.6x10^{12}M^{-1}$  and  $K_T=418M^{-1}$ , with  $\Lambda_o^T=\frac{2}{3}\Lambda_o$ , as done above.

For the above calculation we have used  $\Lambda_{\rm LiClO_4}^{\circ}=115.7\Omega^{-1}~{\rm cm}^2{\rm eq}^{-1}$  in DMC, based on Walden's rule and the results for  ${\rm LiClO_4}$  in propylene carbonate  $\Lambda_{\rm o}=26.75\Omega^{-1}{\rm cm}^2{\rm eq}^{-1}$  and  $\eta=0.0253{\rm p}$ . By using for both  ${\rm LiAsF}_6$  and  ${\rm LiClO}_4$  the data for  $\Lambda_{\rm o}$  in propylene carbonate, having the same  $\sim C=0$  polar group as DMC, it is hoped to achieve a reasonable validity of Walden's rule.

An attempt has been made at this point to see whether the positive deviation of the Fuoss Kraus  $\Lambda g(c)\sqrt{c}$  vs.  $(1-\Lambda/\Lambda_o)c$  plot, a trend observed before  $^{1,2}$  for concentrations higher than  $c\approx 10^{-2} M$  was due to causes other than the ionic strength. It is our contention that the latter is quite low in DMC and that the apparent failure of the theory to represent the data at  $c>10^{-2} M$  is in part due to the inappropriate permittivities and viscosities used in the theoretical expressions. From the microwave portion of the work, we have fitted the static permittivities  $\epsilon$  for LiAsF<sub>6</sub> solutions to the electrolyte concentration c by a cubic polynomial equation which gives by nonlinear regressions

$$\mathbf{r}^2 = 0.9993 \quad \epsilon = 3.11 + 27.479c - 110.340c^2 + 199.25c^3$$
 (II)

valid up to c = 0.25M. In the same concentration range the solution densities

are given by

$$r^2 = 0.99994$$
  $\rho = 1.063 + 0.1879c - 0.2185c^2 + 0.1655c^3$ 

valid within  $\pm 0.001$  g/cm<sup>3</sup>. It is noteworthy to emphasize the point raised above that at 0.25M  $\epsilon = 6.20$  instead of  $\epsilon = 3.11$ , the solvent value. We have then decided to take the variation into account in dealing with the Fuoss-Kraus theory, a concept already expressed years ago by E.A.S. Cavell<sup>11</sup>. In addition, we have corrected the viscosities by the presence of the electrolyte LiAsF<sub>6</sub> by the Einstein equation, as suggested by Fuoss<sup>12</sup>:

$$\eta^{E} = \eta_{o}[1 + \frac{5}{2} \phi] = \eta_{o}[1 + Fc]$$
(III)

where  $\phi$  is the volume fraction  $\phi = \frac{(4\pi R^3/3) Lc}{1000} = \frac{2}{5} Fc$  and  $F=6.308 x 10^{21} R^3$ . R, the radius of the pair (taken as a sphere) has been estimated by the Debye expression  $\tau = \frac{4\pi R^3}{kT} \eta$ ,  $\tau = (2\pi f)^{-1}$  neglecting differences between the decay of the polarization  $\tau_D$  and the real molecular relaxation time  $\tau$  that enter the Debye equation. Similarly,  $\eta \approx \eta_o = 0.00585 p$  has been retained. With  $\overline{f} = 1.7 x 10^9 Hz$ , it results  $R = 3.7 x 10^{-8}$  a value comparable with the sum of the crystallographic radii for LiAsF<sub>6</sub> giving  $R_{\rm cry} = 4.4 x 10^{-8} {\rm cm}$ . One should also point out that we are in complete agreement with Fuoss<sup>12</sup> in that Eq. (III) ought to be used instead of the experimental viscosities. The latter incor-

$$\eta = \eta_0 (1 + S_n \sqrt{c} + Fc)$$

porates the Falkenhagen term  $S_n$ 

expressing the existing velocity gradient in the solution which are absent in the conductance experiment where the solution is at rest as a whole. It results for LiAsF<sub>6</sub> in DMC that F=0.3 and  $\eta^E=\eta_o(1+0.3c)$ . By the aid of Eqs. II and III, we have calculated Eq. I, namely, the g(c) term corrected by  $\epsilon(c)$  and  $\eta^E$ . The data for LiAsF<sub>6</sub> in DMC are reported in Fig. 4. We have then tried to cal-

culate the right side of Eq. (1) from theory, using the expressions by Fuoss-Jagodzinski<sup>14</sup>

$$K_{\rm p} = K_{\rm FJ} = \frac{4\pi L a^3}{3000} e^{-1/2} e^{b}$$

$$K_{\rm T} = K_{\rm FJ}^{\rm T} = \frac{\pi L a^3}{1000} e^{-3/2} e^{b/2}$$
(IV)

Specifically, we have equated Eqs.(IV) to the values of  $K_p$  and of  $K_T$  for LiAsF<sub>6</sub> found experimentally in the low concentration range, namely,  $K_p=8.9\times10^{11}~\mathrm{M^{-1}}$  and  $K_T=445\mathrm{M^{-1}}$  obtaining (with  $\epsilon=3.12$ ) a=6.3x10<sup>-8</sup>cm and a<sub>T</sub>=16.4x10<sup>-8</sup>cm. Without assigning to these parameters physical significance, we have used these numerical values to calculate Eqs. (IV) at all the concentrations using Eq. (II) to evaluate  $\epsilon$ .

The results for LiAsF<sub>6</sub> solutions in DMC are reported in Fig. 4 together with the calculated  $[\Lambda\sqrt{c}~g(c)]_{calc}$  according to the right side of Eq. (1) and also by using  $\Lambda_T^o = \frac{1}{3} \Lambda_o$  as in the original version of the triple-ion theory<sup>3</sup>. In Fig. 4 the solid lines represent these calculated values showing a qualitative trend following the data at variance with the original Fuoss-Kraus theory using  $\epsilon = 3.12$  and  $\eta = 0.00585$ . The introduction of  $\epsilon(c)$  and  $\eta^E$  seems, however, to have overcorrected the  $\Lambda g(s) \sqrt{c}$  data. The results from the microwave data, shown below for LiAsF<sub>6</sub> in DMC, indicate that the ion pairs are not the only complex species present. The Böttcher plot shows a strong concave down curvature indicating lack of proportionality of the relaxation strength  $\epsilon_o - \epsilon_{co}$ , with the total concentration. This, in turn, suggests that the polarization of the solution is not proportional to c and that the total concentration is different from  $\epsilon_p$ , the ion pair concentration. The situation is corrected by the introduction of a quadrupole equilibrium with  $K_q \sim 50 M^{-1}$ .

We have applied the same criterion to the conductance data of LiAsF<sub>6</sub> in

DMC, expressing the total concentration by the two major species present (free ions and triple ions are in minor quantities)

$$c = (AB) + 2(A_2B_2) = c_p + 2c_p^2K_q$$

and using  $c_{\rm p}$  rather than c in the Fuoss-Kraus definition

$$A +B \rightleftharpoons AB + B \rightleftharpoons AB_2$$
  
+  $A \rightleftharpoons A_2B$ 

with  $(A)=(B)=\alpha c_p$ ;  $(AB)=c_p(1-\alpha-3\alpha_T)$ ;  $(AB_2)=(A_2B)=\alpha_T c_p$  leading to the usual expression

$$\Lambda g(c)\sqrt{c_p} = \frac{\Lambda_o}{\sqrt{K_p}} + \frac{\Lambda_o^T K_T}{\sqrt{K_p}} (1 - \frac{\Lambda}{\Lambda_o})c_p$$
 (V)

which differs from Eq. (I) only by the presence of  $c_p$  instead of c. Fig. 5 reports the left and right side of equation (V) depicted, the former by the experimental point, the latter by the solid line. Although the data for  $\Lambda_o^T = \frac{1}{3}\Lambda_o$  are overcorrected in the lower portion of the curve and undercorrected in the upper portion, the general qualitative trend is followed up to  $c\approx 0.1 M$ , a large improvement over the original calculations using  $\epsilon=3.12$  and  $\eta=0.00585$ , the solvent properties.

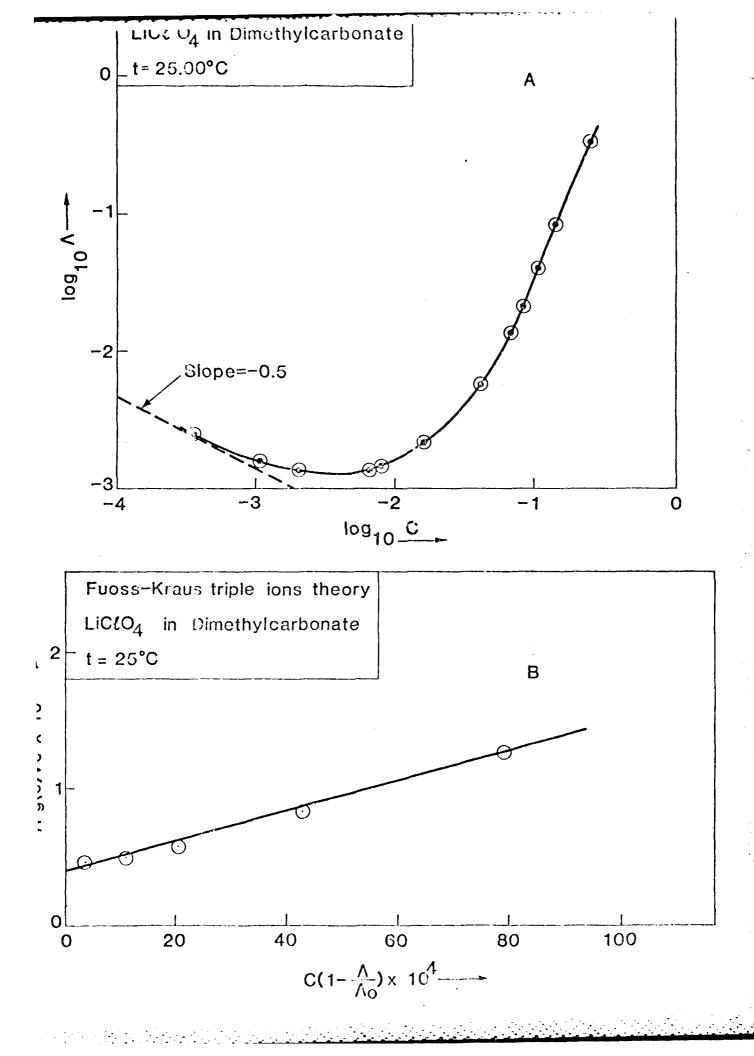
The same sequence of calculations has been applied to the LiClO<sub>4</sub> data. The permittivity is expressable in terms of the concentration of LiClO<sub>4</sub> by the expression  $\epsilon = 3.12 + 7.833c + 47.228c^2 - 125.61c^3$  with  $r^2 = 1.0000$ . The density of the solutions can be expressed by the relation  $\rho = 1.063 - 0.024856m + 1.0607m^2 - 2.4134m^3$  with m the molality of the solutions and  $r^2 = 0.99993$ . The average lower decay time of the polarization of the solutions taken to be approximately equal to the relaxation time  $\tau = (2\pi f)^{-1} = (2\pi x 1.3x 10^9)^{-1} = 122.4x 10^{-12}$  seconds which, by the aid of the Debye expression  $\tau = (4\pi R^3/kT)\eta$  gives  $R = 4.09x 10^{-8}$ cm. This value intro-

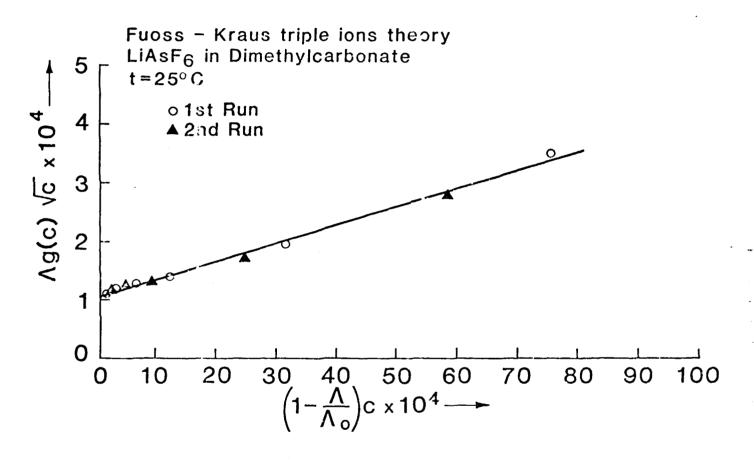
duced into the Einstein relation  $\phi=(4\pi\,\mathrm{R}^3/3)\,\mathrm{Lc}/1000=(2/5)\mathrm{Fc}$  gives  $\mathrm{F}=0.43$  and  $\eta^{\mathrm{E}}{=}\eta_{\mathrm{o}}\,(1+0.43\mathrm{c})$ .

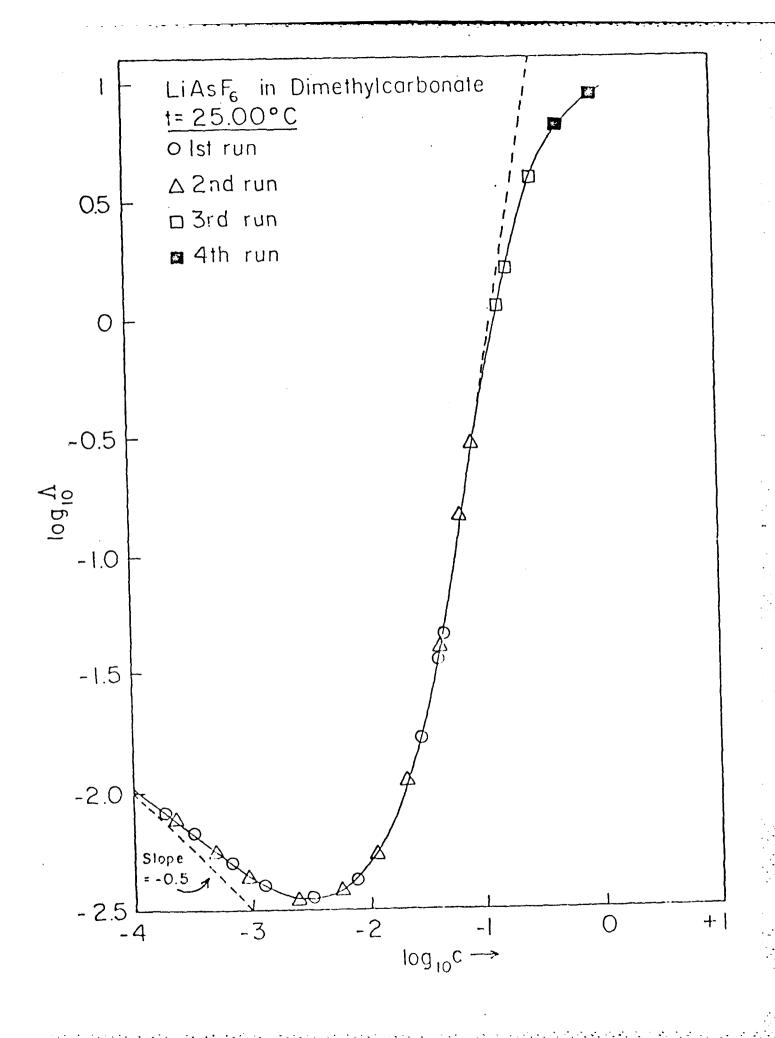
The calculation has been then applied using equation (1) as for the case of the LiAsF<sub>6</sub> data, using the  $\epsilon(c)$  and  $\eta^E$  data. The results of this calculation are depicted in Fig. 6 where the solid lines correspond to the theoretical  $\Lambda$  g(c) $\sqrt{c}$ , calculated by the aid of equations (V)  $\Lambda_o^T = \frac{2}{3}\Lambda_o$  and  $\Lambda_o^T = \frac{1}{3}\Lambda_o$ . The values of a = 5.8x10<sup>-8</sup>cm and a<sub>T</sub> = 16.8x10<sup>-8</sup>cm have been used based on the fit of the experimental  $K_p = 8.6x10^{12} M^{-1} K_T = 418 M^{-1}$  from the low concentration data. From Fig. 6 the same consideration as for LiAsF<sub>6</sub> hold, namely, the agreement of the calculated and experimental data although qualitative, encompasses a larger concentration range than in the original theory using  $\epsilon = 3.12$  and  $\eta = 0.00585p$ .

The difference from the LiAsF<sub>6</sub> case is that there is no need of introducing a quadrupole constant, as evidenced also by the microwave data showing no evidence of quadrupole complexation for LiClO<sub>4</sub>, the Böttcher plot being linear. In the above calculation of  $\Lambda$  g(c) $\sqrt{c}$  the best fit is obtained by the position  $\Lambda_0^T = \frac{1}{3}\Lambda_0$  as in the original Euoss-Kraus theory. One could surmise that by adjusting  $K_p$ ,  $K_T$ , and  $K_q$  (for LiAsF<sub>6</sub>) the fit may become better. Here, however, we wish only to stress the concept that by using the information from the microwave experiments (that the permittivity of the solution changes) and by correcting viscosities, a significant improvement over the concentration range usable by the conductance theory can be obtained.

In other words, at very low permittivities, where very few ions are present, the failure of the theory is not due to ionic strength effects, but rather to the neglect of the effect of the presence of large quantities of neutral species and their altering the permittivity  $\epsilon$  and viscosity  $\eta$ . Improvements on the theory







Böttcher function  $\phi(\epsilon) = (\epsilon_{o} - \epsilon_{oo_1}) \frac{2\epsilon_{o} + 1}{3\epsilon_{o}}$  vs. c and vs. Fig. 9

$$c_{p} = \frac{-1 + \sqrt{8K_{q}c + 1}}{4K_{q}}$$

 $c_p = \frac{-1+\sqrt{8K_qc+1}}{4K_q}$  for LiAsF in DMC at t = 25°C.  $K_q$  is the dimerization constant for ion pairs to quadrupoles (or dimers).

Böttcher function  $\phi(\epsilon) = (\epsilon_0 - \epsilon_{00_1}) \frac{2\epsilon_0 + 1}{3\epsilon_0}$  vs. c for LiClO<sub>4</sub> in Fig. 10 DMC at t = 25°C.

#### List of Figures

Fig. 1  $\log_{10}\Lambda$  vs.  $\log_{10}c$  for LiAsF<sub>6</sub> in DMC at 25°C.  $\Lambda$  is the equivalent conductivity, c is the molar concentration.

Fig. 2  $\Lambda g(c)\sqrt{c}$  vs.  $(1-\frac{\Lambda}{\Lambda_0})c$  for LiAsF<sub>6</sub> in DMC at  $c \le 0.01$ M.

Fig. 3a  $\log_{10}\Lambda$  vs.  $\log_{10}c$  for DMC at  $t = 25^{\circ}C$ .

Fig. 3b  $\Lambda g(c)\sqrt{c}$  vs.  $(1-\frac{\Lambda}{\Lambda_0})c$  for LiClO<sub>4</sub> in DMC at  $c \leq 0.01$ M.

Fig. 4  $\Lambda g(c)\sqrt{c}$  vs.  $(1-\frac{\Lambda}{\Lambda_o})c$  for LiAsF<sub>6</sub> in DMC at  $c \leq 0.07M$ . g(c) has been calculated with  $\epsilon(c)$  and  $\eta^E$  (see text).

Fig. 5  $\Lambda \, g(c_p) \sqrt{c_p} \, \text{ vs. } (1 - \frac{\Lambda}{\Lambda_o}) c_p \, \text{ for LiAsF}_6 \, \text{ in DMC at 25°C.} \, c_p \, \text{ has}$  been calculated from the expression  $c = c_p + 2 K_q c_p^2$  with  $K_q = 50 M^{-1}$ . Also  $\epsilon(c)$  and  $\eta^E$  have been used for the calculation of  $g(c_p)$ .

Fig. 6  $\Lambda g(c)\sqrt{c}$  vs.  $(1-\frac{\Lambda}{\Lambda})c$  for LiClO<sub>4</sub> in DMC at  $c \le 0.07M$ . g(c) has been calculated with  $\epsilon(c)$  and  $\eta^{E}$  (see text).

Fig. 7a  $\epsilon'$  vs. f and  $\epsilon_{\rm d}{''}=(\epsilon''-\epsilon_{\rm x}{''})$  vs. f for LiAsF<sub>6</sub> 0.25M.

Fig. 7b Cole-Cole plot:  $\epsilon_d{''}=(\epsilon''-\epsilon_x{''})$  vs.  $\epsilon'$  for LiAsF<sub>6</sub> 0.25M in DMC.

Fig. 8a  $\epsilon'$  vs. i and  $\epsilon''$  vs. f for LiAsF<sub>6</sub> 0.15M in DMC; t=25°C.

Fig. 8b Cole-Cole plot of  $\epsilon_d{''}=(\epsilon''-\epsilon_x{''})$  vs.  $\epsilon'$  for LiAsF<sub>6</sub> 0.15M in DMC.

#### TABLE II

Dielectric Relaxation Parameters and Electrical Conductivity X for LiAsF<sub>6</sub> and LiClO<sub>4</sub> in Dimethylcarbonate at 25°C at the Concentrations Investigated.

#### LiAsF<sub>6</sub>

c	$\epsilon_{_{ m O}}$	<b>€</b> ○○ 1	€ <sub>002</sub>	f <sub>l</sub> (GHz)	f <sub>2</sub> (GHz)	$(\Omega^{-1}cm^{-1})$	læ'la	1/e" b
0.25	6.20	3.50	2.50	1.6	22	$7.38 \times 10^{-4}$	0.095	0.06
0.15	5.40	3.40	2.45	1.8	22	$1.66 \times 10^{-4}$	0.04	0.05
0.10	5.00	3.30	2.40	1.6	22	$3.98 \times 10^{-5}$	0.08	0.05
0.05	4.20	3.20	2.40	1.8	22	$2.94 \times 10^{-6}$	0.04	0.02
LiClO <sub>4</sub>	<u>.</u>							
0.29	6.30	3.40	2.45	1.4	22	$1.24 \times 10^{-4}$	0,026	0.041

 $<sup>3.22 \</sup>times 10^{-5}$ 0.19 22 0.053 5.50 3,35 2.45 1.3 0.047 0.10<sup>b</sup>  $3.46 \times 10^{-6}$ 4.25 18 0.64 3.30 2.40 0.28 1.2  $^{0}\mathbf{p}$ 3.12 2.35 22 0.35 0.22

a  $|\Lambda \varepsilon'|$  and  $|\Lambda \varepsilon'|$  the absolute average deviations ( $\varepsilon'$  calc  $-\varepsilon'$  exp) and  $(\varepsilon''$  calc  $-\varepsilon''$  exp).

<sup>&</sup>lt;sup>b</sup>Saar, D., Brauner, J., Farber, H., Petrucci, S., J. Phys. Chem. <u>82</u> (1978) 5451.

#### TABLE I (Continued)

Equivalent Conductance h and Molar Concentration c for LiClO<sub>4</sub> in Dimethylcarbonate;  $t=25^{\circ}C$ .

c x 10 <sup>4</sup>	٨
(M)	$(\Omega^{-1} \operatorname{cm}^2 \operatorname{eq}^{-1})$
Run No. 1 3.5683	0.0025203
10.720	0.0015583
20.323	0.0013282
42.937	0.0013181
78.760	0.0014885
159.865	0.0021431
412.97	0.0058785
696.65	0.013938
863.82	0.021501
1059.4	0.041264
Run No. 2 1417.4	0.084089
2488.3	0.3368

a)Both runs were performed with a cell of constant  $K_c = 0.1156 \text{ cm}^{-1}$ .

TABLE I

Equivalent Conductance A and Molar Concentration c for LiAsF<sub>6</sub> in Dimethylcarbonate; t=25°C

Ru	in No. 1	Run No. 2		
$c \times 10^4$ (M)	$(\Omega^{-1} \operatorname{cm}^{2} \operatorname{eq}^{-1})$	$c \times 10^4$ (M)	$(\Omega^{-1} \operatorname{cm}^2 \operatorname{eq}^{-1})$	
1.8881	0.008235	2.2480	0.007718	
3.2683	0.006724	4.9147	0.005702	
6.669	0.005031	9.2272	0.004404	
12.282	0.004052	24.829	0.003526	
31.446	0.003626	58.403	0.003832	
75.513	0.004278	113.06	0.005421	
142.59	0.006703	216.50	0.01102	
281.56	0.016853	427.08	0.03960	
412.96	0.036562	692.08	0.1442	
450.84	0.045138	884.22	0.2935	
Run No. 3		Run No. 4		
1511.9	1.1488	5127	6.8609	
1807.4	1.6670	10,090	9.002	
3110.5	3.9865			

Runs 1, 2, and 3 were performed with a cell of constant  $K_c = 0.1156 \text{ cm}^{-1}$ , Run 4 with a cell of constant  $K_c = 0.2794 \text{ cm}^{-1}$ .

- 16. Menard, D., Chabanel, M., J. Phys. Chem (1975) 79, 1081.
- Saar, D. Brauner, J., Farber, H., Petrucci, S., J. Phys. Chem. (1978) 82,
   1943.
- 18. Paoli, M., Lucon, M., Chabanel, M., Spectrochima Acta (1979) 354, 593.

#### References

- 1. Farber, H., Irish, D. E., Petrucci, S., J. Phys. Chem. (1983) 87, 3515.
- Delsignore, M., Maaser, H. E., Petrucci, S., J. Phys. Chem. (1984) 88,
   2405.
- Saar, D., Brauner, J., Farber, H., Petrucci, S., J. Phys. Chem. (1972) 82,
   545.
- Maaser, H. E., Delsignore, M., Newstein, M., Petrucci, S., J. Phys. Chem. (1984) 88, 5100.
- Petrucci, S., Hemmes, P., Battistini, M., J. Am. Chem. Soc. (1967) 89, 5552.
- 6. Farber, H., Petrucci, S., J. Phys. Chem. (1975) 79, 1221.
- 7. Farber, H., Petrucci, S., J. Phys. Chem. (1981) 85, 1396.
- Lind, J. E., Zwolenik, J. J., Fuoss, R. M., J. Am. Chem. Soc. (1959) 81, 1557.
- 9. Fuoss, R. M., Kraus, C. A., J. Am. Chem. Soc. (1933) 55, 2387.
- 10. Salomon, M., Plichta, E. J., Electrochim. Acta. 29 (1984) 731.
- Cavell, E. A. S., Knight, P. C., Zeit. für Physik. Chem. N. F. (1968) 57,
   3.
- 12. Fuoss, R. M., Accescina, F., Electrolytic Conductance Intersci. N.Y., 1959, page 234.
- Falkenhagen, H., Dole, M., Z. Physik. Chem. (1929) 6, 159; Falkenhagen,
   H., Physik. Z. (1931) 32, 365, 745.
- 14. Jagodzinski, P., Petrucci, S., J. Phys. Chem. (1974) 78, 917.
- Böttcher, C. F., "Theory of Electrical Polarization," Elsevier Amsterdam,
   1973.

ence of a centrosymmetrical quadrupole 18

$$S = C = N$$
 $N = C = S$ 

which by symmetry would have a zero dipole moment in accord to our contention for LiSCN in DMC and DEC.

Figure 10 reports the Böttcher plot, according to Eq. (VII) for the dielectric data of LiClO<sub>4</sub> in DMC. Linear regressions giving 50% statistical weight to the origin gives  $r^2 = 0.995$  slope = 7.413 from which one calculates the apparent dipole moment  $\mu = 11.0 \times 10^{-18}$  esu cm. By taking a rigid sphere model (consistent with having neglected the polarization-reaction field term  $(1-\alpha f)^2$  gives  $\mu = \text{ae}$  and  $a = 2.3 \times 10^{-8} \text{cm}$  giving a strong indication of contact species for LiCLO<sub>4</sub>.

It is noteworthy that no curvature of the Böttcher plot is visible, at variance with the case of  $\text{LiAsF}_6$  in DMC, indicating apparent absence of quadrupoles for  $\text{LiClO}_4$  in DMC. This is somewhat surprising in view of  $\text{K}_p(\text{LiClO}_4 > \text{K}_p(\text{LiAsF}_6))$ . One could, however, invoke the smaller dipole moment of  $\text{LiClO}_4$ ) with respect to  $\text{LiAsF}_6$ , hence the smaller dipole-dipole energy  $\mu_1\mu_2\cos\theta/\epsilon r^3$  (with  $\theta$  the angle of mutual orientation) as the reason for the undetectable  $\text{K}_q$  for the case of  $\text{LiClO}_4$ .

 $r^2=0.990$  Int = 0.017, slope = 42.89 for  $K_q=50~M^{-1}$ . One ought to add, however, that the optimum fit is rather insensitive on  $K_q$ , a value of  $K_q=30~M^{-1}$  giving almost as good a result as  $K_q=50~M^{-1}$ . Using  $K_q=50~M^{-1}$ , the apparent dipole moment results  $\mu=26.5~x~10^{-18}$  esu cm, namely,  $a_\mu=5.5x\,10^{-8}$ cm, taking a rigid sphere model  $\mu=$  ae for LiAsF<sub>6</sub> in DMC. With  $K_q=30M^{-1}$ ,  $r^2=0.990$ , Int = 0.063, S=33.35,  $\mu=23.3~x~10^{-8}$  esu cm and  $a_0=4.9~x~10^{-8}$  cm

In either case one may be led to the conclusion that  $a_{\mu}$  is of the order of magnitude of the sum of the crystallographic radii. Values for the dimerization constants have been calculated by Chabanel et al., <sup>16</sup> from static dielectric data for LiBr, LiSCN and AgClO<sub>4</sub>. The calculation was based on assuming that the static dielectric increments over the solvent were due to both monomer pairs and dimers or quadrupoles

$$\Delta \epsilon = \delta_1(AB) + \delta_2(A_2B_2)$$

implying that the quadrupoles are polar and that  $\delta_2 \neq 0$ . In fact, it was reported that  $\delta_2 = 1.8$  for LiBr,  $\delta_2 = 10.8$  for LiSCN and  $\delta_2 = 8.6$  for AgClO<sub>4</sub> giving quadrupole constants  $K_q(\text{LiBr}) = 90 \, \text{M}^{-1}$ ,  $K_q(\text{LiSCN}) = 20 \, \text{M}^{-1}$  and  $K_q(\text{AgCLO}_4) = 45 \, \text{M}^{-1}$ . For LiClO<sub>4</sub> the effect of quadrupoles was undetectable. Later, however, it was found<sup>17</sup> that for both dimethylcarbonate and diethylcarbonate solvents, for LiSCN and LiClO<sub>4</sub>, the microwave complex permittivity data extrapolated to static values  $\epsilon_0$ 's comparable with the data by Chabanel et al. As the microwave data were interpretable by a single Debye relaxation which was assigned to the rotation of only polar ion-pairs, one had to conclude 17 that the dimers were apolar. Hence, the assumptions on the  $\delta_2$ 's made by Chabanel and the calculated  $K_q$ 's had to be incorrect. It is also noteworthy that 1R spectra in ethers in the 2040cm<sup>-1</sup> range indicated the pres-

where  $|\Delta\epsilon'| = |\epsilon'(\text{calc}) - \epsilon'(\text{exp})|$  and  $|\Delta\epsilon''| = |\epsilon''(\text{calc}) - \epsilon''(\text{exp})|$  are the absolute values of the deviations.<sup>3</sup> We have already shown in the conductance section dealing with the LiAsF<sub>6</sub> data that the value of a obtained from the decay time of the polarization  $\tau$  is comparable to the sum of the crystallographic radii, at least as an order of magnitude. In order to gain more structural information on the system, we have plotted the Bötcher function<sup>15</sup>

$$\epsilon_{o} - \epsilon_{oo_1} = \frac{4\pi \operatorname{Lex} 10^{-3}}{(1 - \alpha f)^2} \frac{\mu^2}{3kT} \frac{3\epsilon_o}{2\epsilon_o + 1}$$
 (VII)

in the form  $(\epsilon_0 - \epsilon_{0.0})$   $\frac{2\epsilon_0 + 1}{3\epsilon_0}$  vs. c for LiAsF<sub>6</sub> in DMC. Neglecting the polarizability  $\alpha$ , reactor field factor of term  $(1 - \alpha f)^2$  of the order of unity, one would expect a straight line. In fact in Fig. 9 one may see a strong concave down curvature.\* This behavior becomes obvious if one realizes that in DMC one ought to expect much higher dimerization of pairs than in the DME and 2MTHF ethers studied so far. This is because of the lower permittivity of DMC.

If one accepts the idea that polar dimers are formed, ruled by the equilibrium  $2AB \rightleftharpoons (A_2B_2)$  and  $K_q = \frac{(A_2B_2)}{(AB)^2}$  then by combining the expressions

$$C = (AB) + 2(A_2B_2)$$

$$K_{q} = (\Lambda_{2}B_{2})/(\Lambda B)^{2}$$

 $c_p=AB$  can be calculated for tentative values of  $K_q$ . Linear regressions of  $\phi(\epsilon)$  vs.  $c_p$  should give the best straight line for the best  $K_q$ . The calculation has been done and shown in Fig. 9 leading to

$$\phi(\epsilon) = (\epsilon_{0} - \epsilon_{00_{1}}) \frac{2\epsilon_{0} + 1}{3\epsilon_{0}}$$

vs. c gives  $r^2 = 0.0008$ 

$$\phi(\epsilon) = -0.002 + 19.534c - 91.273c^2 + 177.023c^3$$

giving 50% statistical weight to the origin

<sup>\*</sup> Nonlinear regression of

will have to be made by trying to incorporate these changes, nowadays measurable by modern tools as microwave spectrometry for  $\epsilon$ , rather than trying to improve on the mathematical treatment. This to date, expressed by the Onsager-Fuoss-Kraus various editions of the theory<sup>12</sup> remains an unsurpassed legacy of ingenuity, elegance and rigor.

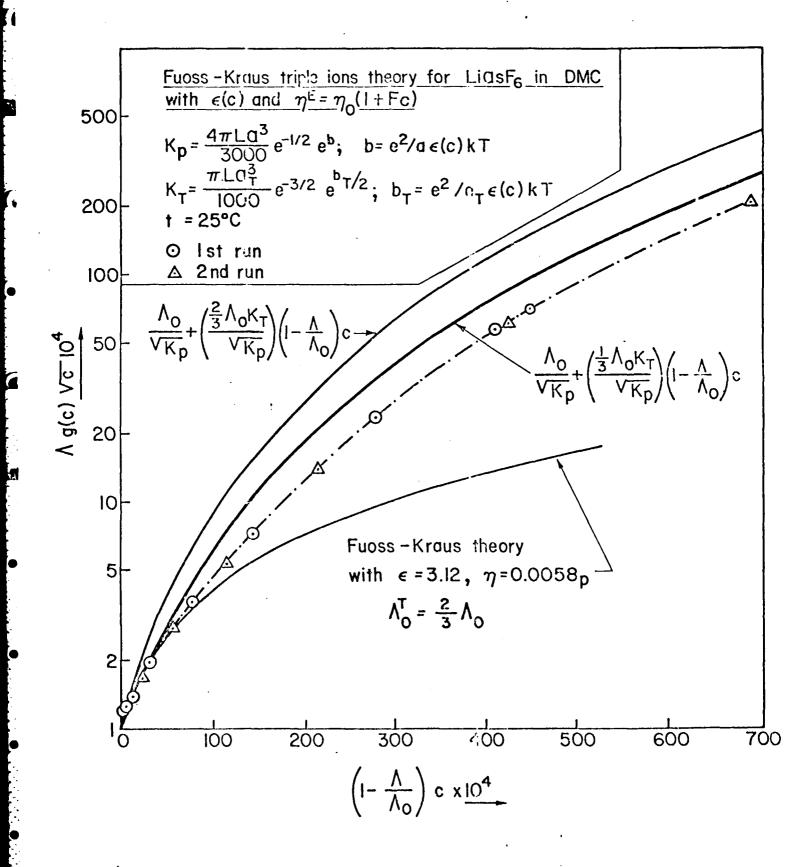
#### b) Microwave Complex Permittivities

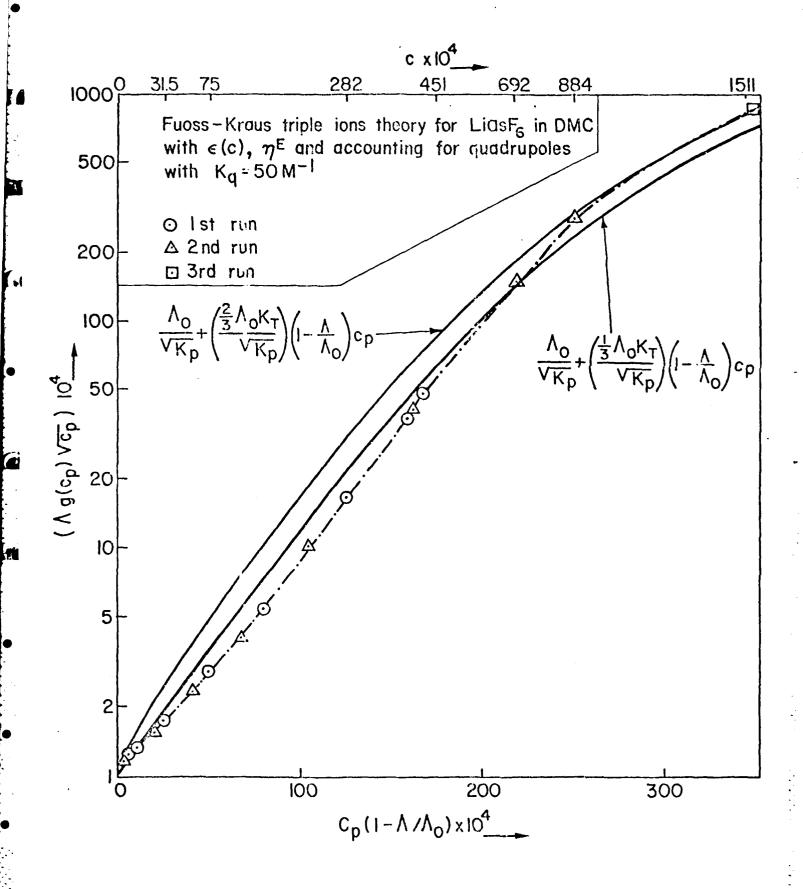
Figures 7 and 8 show representative plots of the coefficient of the real part  $\epsilon'$  and of the imaginary part  $\epsilon''$  of the complex permittivity  $\epsilon_d^* = \epsilon' - J\epsilon_d''$ , plotted vs. the frequency f for LiAsF<sub>6</sub> and LiClO<sub>4</sub> in DMC. The solid lines are the sum of two Debye single relaxation processes according to the functions

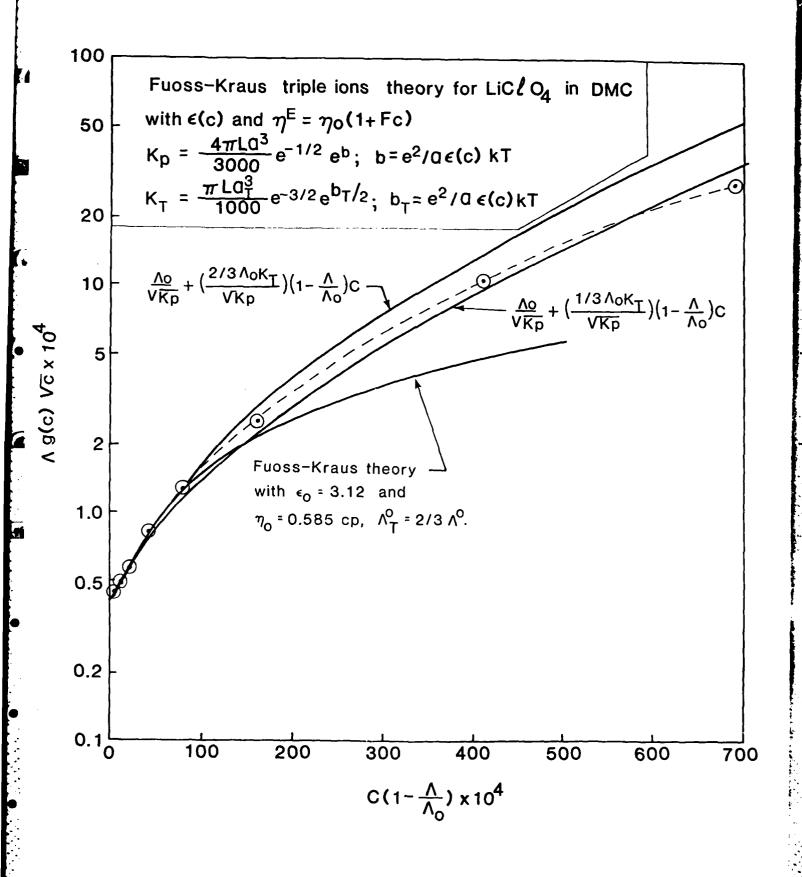
$$\epsilon' = \frac{\epsilon_0 - \epsilon_{00_1}}{1 + (f/f_1)^2} + \frac{(\epsilon_{00_1} - \epsilon_{00_2})}{1 + (f/f_2)^2} + \epsilon_{00_2}$$
(VI)

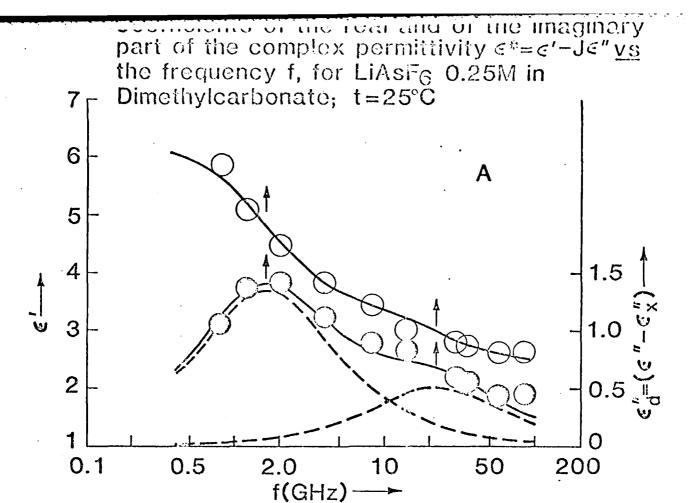
$$\epsilon_{d}^{"} = (\epsilon_{o} - \epsilon_{oo_{1}}) \frac{f/f_{1}}{1 + (f/f_{1})^{2}} + (\epsilon_{oo_{1}} - \epsilon_{co_{2}}) \frac{f/f_{2}}{1 + (f/f_{2})^{2}}$$

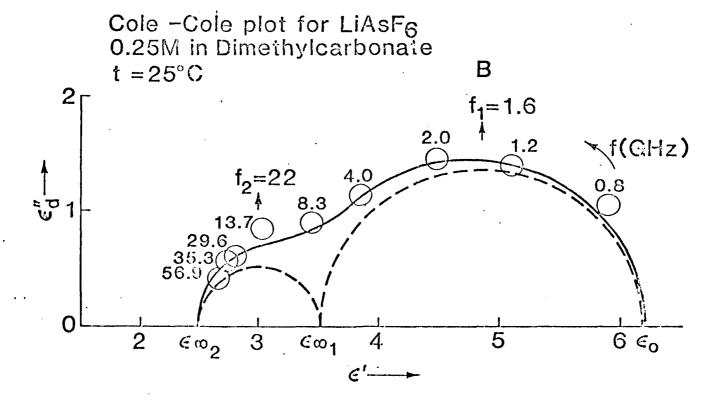
with  $\epsilon_0, \epsilon_{00_1}, \ \epsilon_{00_2}, f_1, f_2$  relaxation parameters.  $\epsilon_0$  is the static permittivity of the solution ( $\epsilon_0 - \epsilon_{00}$ ) and ( $\epsilon_{00_1} - \epsilon_{00_2}$ ) the respective relaxation strength of solute and solvent,  $f_1$  and  $f_2$  the relaxation frequencies associated with the solute and the solvent in the solution.  $\epsilon_{00_1}$  should extrapolate at zero electrolyte concentration to the static permittivity of the pure solvent. In Figs. 7 and 8 the Cole-Cole plots of the quantities  $\epsilon_d''$  vs.  $\epsilon'$  are also depicted. The solid lines correspond to the sum of two Debye processes according to Eqs. (VI). In the above,  $\epsilon_d''$  is the total dielectric loss  $\epsilon''$  subtracted of the contribution due to the conductance  $\epsilon_X'' = 1.8 \times 10^{12} \text{N/f}$  with X the specific conductance of the solutions  $\Omega^{-1} \text{cm}^{-1}$ ). In Table II the dielectric relaxation parameters are reported together with the conductivity X. Eqs. (VI) have been fitted to the data by a trial and error procedure that minimize the summations  $\sum |\Delta \epsilon''| + \sum |\Delta \epsilon''|$ 

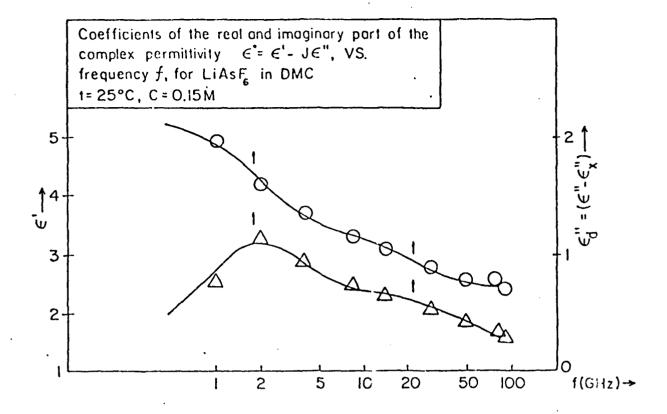


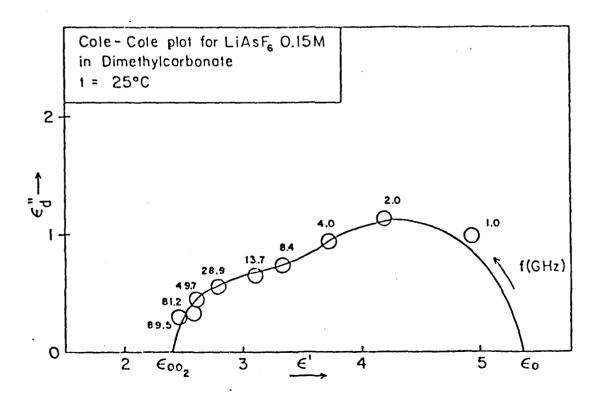


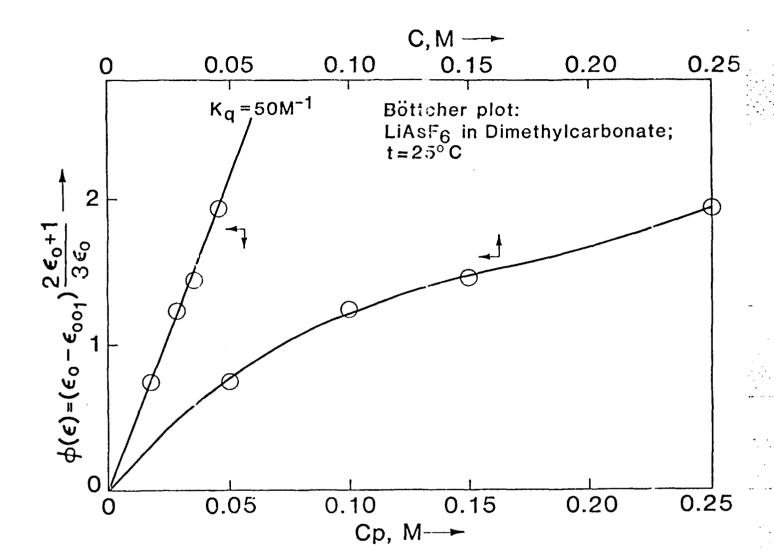


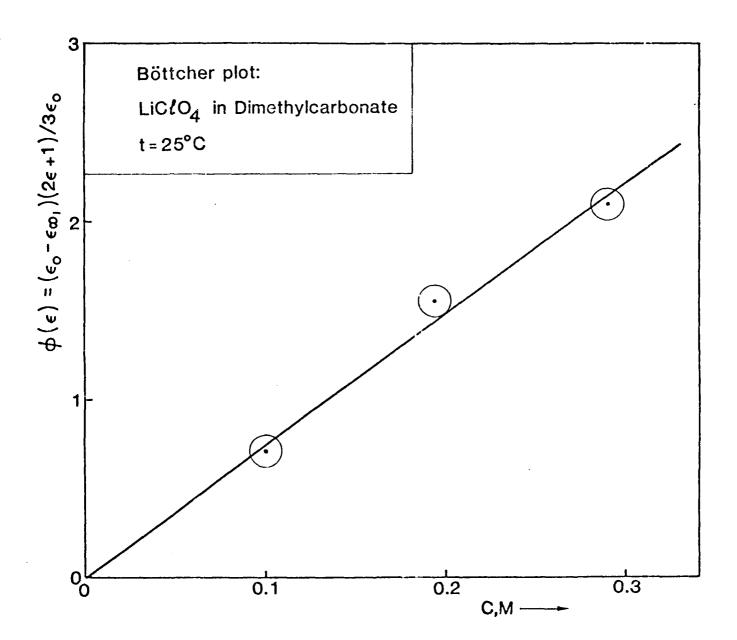












FERRODUCED AT GOVERNMENT LICHLINSE

# END

## FILMED

4-85

DTIC